ARTICLES

Journal of Semiconductors
(2023) 44, 114101
doi: 10.1088/1674-4926/44/11/114101

Development of a simple two-step lithography fabrication process for resonant tunneling diode using air-bridge technology

Swagata Samanta[1, 2, †], Jue Wang[2], and Edward Wasige[2]

[1]Department of Electronics and Communication Engineering, SRM University-AP, Andhra Pradesh, India
[2]School of Engineering, University of Glasgow, Glasgow G12 8LT, UK

Abstract: This article reports on the development of a simple two-step lithography process for double barrier quantum well (DBQW) InGaAs/AlAs resonant tunneling diode (RTD) on a semi-insulating indium phosphide (InP) substrate using an air-bridge technology. This approach minimizes processing steps, and therefore the processing time as well as the required resources. It is particularly suited for material qualification of new epitaxial layer designs. A DC performance comparison between the proposed process and the conventional process shows approximately the same results. We expect that this novel technique will aid in the recent and continuing rapid advances in RTD technology.

Key words: air-bridge; indium phosphide; microfabrication; resonant tunneling diode

Citation: S Samanta, J Wang, and E Wasige, Development of a simple two-step lithography fabrication process for resonant tunneling diode using air-bridge technology[J]. *J. Semicond.*, 2023, 44(11), 114101. https://doi.org/10.1088/1674-4926/44/11/114101

1. Introduction

Resonant tunneling diodes (RTDs) have received a lot of attention due to their structural simplicity, ultra-high frequency capability, low power consumption, and their ability to operate at room temperature[1−6]. They are widely applied in micro/nanoelectronics and communications (oscillators, logic circuits, transmitter, wireless link), optoelectronics (phototransistor, photodetector, light emitting diode, optical modulator, single photon detector), and recently in neuromorphic applications[7−21]. RTDs typically consist of a quantum well sandwiched in between two barriers and work on the principle of quantum tunneling effect. Negative differential resistance (NDR), which is a unique characteristic of this semiconductor device, allows them to be applicable in a wide range of areas (as mentioned above). Research on RTDs commenced with the start of the theoretical studies on tunneling phenomenon in a superlattice by Leo Tsu and Raphael Esaki in the 1970s and along with Chang in 1974[22−24]. These RTDs were experimentally demonstrated for the first time in 1974 at liquid nitrogen temperature, where the NDR region was observed in the current voltage (*I*–*V*) characteristics; however, the first room temperature experiment was only conducted in 1985[24, 25].

The conventional fabrication process for RTDs requires six lithography steps and mainly employs the polyimide process[26, 27] for passivation. The first step here is the deposition of top metal contact, followed by the top mesa step (where etching is conducted until the emitter layer). The bottom mesa step, which etches till the substrate, is followed by the formation of a bottom metal contact. A polyimide is used in the passivation step. The use of a polyimide passivation layer is essential to protect the device from external contaminants and to prevent unwanted surface recombination effects that can degrade the device performance at the cost introducing parasitic capacitance, which is crucial for high frequency applications. Finally, via-opening and metal bond pads deposition completes the fabrication process. Opening of the top contact (i.e., via-opening) after passivation is a critical step in enabling an electrical connection between top contact and bond pad, and is a challenging step, especially while fabricating the nanoscale dimension RTDs. The air-bridge approach overcomes the critical top-contact connection step of the conventional processes, where a suspended air-bridge structure is made that connects the top metal and the bond pad. Although similar fabrication approaches have been reported in the literature[28−32], they all require at least four lithography steps.

In this work, we report details of the process and compare the DC performance of a 4×4 μm^2 DBQW RTD using the proposed air-bridge technique with that from similarly sized devices made from the same epitaxial wafers but fabricated using the conventional polyimide process. DC characterization shows that both these processes have nearly the same performance.

This paper is organized as follows: Section 2 describes the RTD device epi-structure and fabrication details. Section 3 deals with the device characterization, while concluding remarks and future perspectives are discussed in Section 4.

2. Device structure and fabrication

The epi-structure of the RTD device used in this work was grown by MBE (molecular beam epitaxy) on a semi-insulating (SI) indium phosphide (InP) substrate. This structure,

Correspondence to: S Samanta, swagata.s@srmap.edu.in
Received 9 APRIL 2023; Revised 21 MAY 2023.
©2023 Chinese Institute of Electronics

Thickness	Material	Doping	
40 nm	$In_{0.53}Ga_{0.47}As$	3×10^{19} cm^{-3}	← collector
160 nm	$In_{0.53}Ga_{0.47}As$	2×10^{18} cm^{-3}	
25 nm	$In_{0.53}Ga_{0.47}As$	2×10^{16} cm^{-3}	
1.5 nm	$In_{0.53}Ga_{0.47}As$	(undoped)	
1.4 nm	AlAs	(undoped)	← barrier (RTD)
4.5 nm	$In_{0.53}Ga_{0.47}As$	(undoped)	← well (RTD)
1.4 nm	AlAs	(undoped)	← barrier (RTD)
1.5 nm	$In_{0.53}Ga_{0.47}As$	(undoped)	
25 nm	$In_{0.53}Ga_{0.47}As$	2×10^{16} cm^{-3}	
25 nm	$In_{0.53}Ga_{0.47}As$	2×10^{18} cm^{-3}	
200 nm	$In_{0.53}Ga_{0.47}As$	1×10^{19} cm^{-3}	
200 nm	$In_{0.53}Ga_{0.47}As$	1×10^{19} cm^{-3}	← emitter
370 μm	Semi-insulating InP		← substrate

Fig. 1. InGaAs/AlAs RTD epistructure.

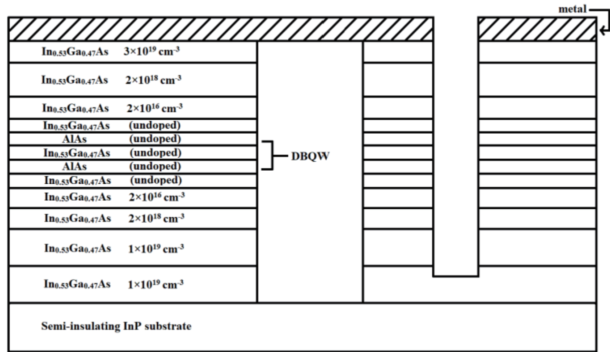

Fig. 2. Cross-section of the designed RTD device.

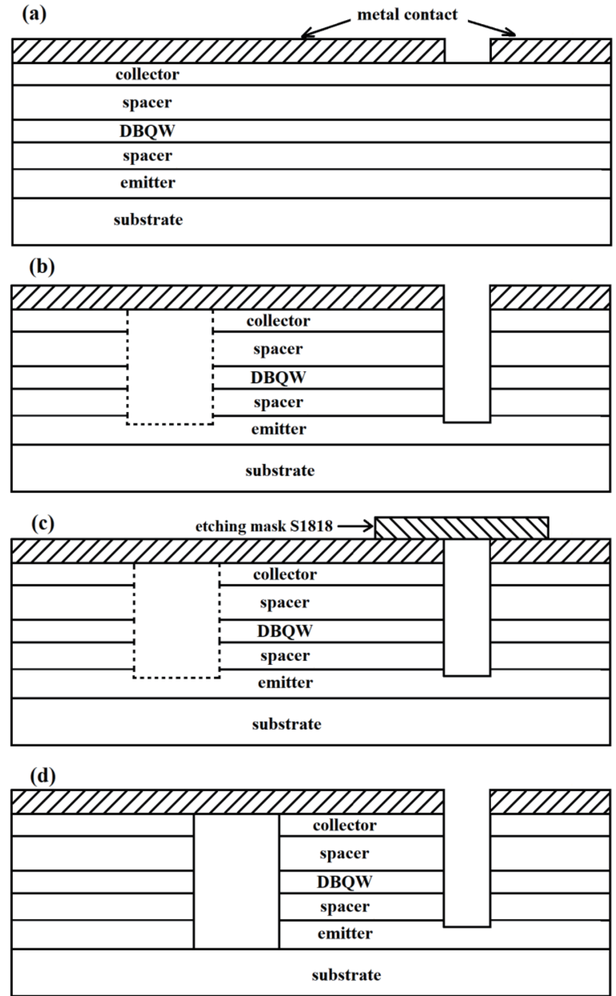

Fig. 3. Fabrication process flow (a) emitter and collector contact patterning by using electron beam lithography, (b) wet etch to bottom contact layer, (c) air-bridge patterning by using photolithography, (d) wet etch to substrate (due to anisotropic etching, air-bridge is formed) and stripping-off etching mask S1818.

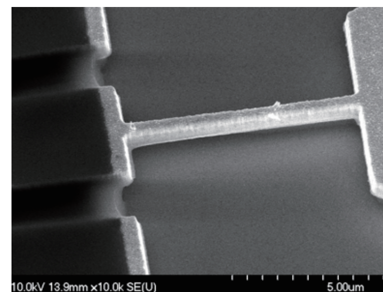

Fig. 4. Scanning electron microscopic view of the fabricated RTD device with air-bridge.

shown in Fig. 1, consists of a 4.5 nm indium gallium arsenide ($In_{0.53}Ga_{0.47}As$) quantum well that is sandwiched in between 1.4 nm AlAs barriers; the barriers being surrounded by undoped and lightly doped $In_{0.53}Ga_{0.47}As$ spacer layers ($In_{0.53}Ga_{0.47}As$) on both sides. The collector and emitter layers are made of heavily doped $In_{0.53}Ga_{0.47}As$ material doped with silicon. The devices were fabricated by both photolithography and electron beam lithography. Only two lithography steps were required. Fig. 2 shows the cross section of the device. The emitter and collector contact pads were patterned by using electron beam lithography. The metal pattern was then used as a mask for an orthophosphoric based chemical wet etch to the emitter (bottom) contact layer. Next, the collector pad and RTD were protected with photoresist by using photolithography, followed by a final chemical wet etching step to the substrate. Fig. 3 illustrates the process steps, while Fig. 4 shows the scanning electron microscopic view of the fabricated RTD device showing the air-bridge, which is 5 μm wide and 55 μm long.

3. Device characterization

Performance analysis for the fabricated RTD device is done by DC characteristics measurement. The setup is shown in Fig. 5. A semiconductor device parameter analyzer (Keysight B1500A) was used for DC characterization of the device. The bond pads (60×100 μm^2) are connected to the terminals on the parameter analyzer through two DC probes. The measured I–V characteristic of the 4×4 μm^2 RTD at room temperature is shown in Fig. 6(a). The device exhibits a peak-to-valley current ratio of 3 and peak current density of 143 kA/cm^2. The detailed results, including the comparison with conventionally fabricated devices are shown in Table 1 and Fig. 6. It can be seen that both processes have nearly the same performance. Thus, the proposed simple RTD fabrication process is robust and has comparable performance with the conventional polyimide process.

The performance of 4×4 μm^2 RTD device (fabricated by our proposed air-bridge process) is also compared with the available literature (based on air-bridge work) and the results are given in Table 2. It should be noted that the comparison here is made with the available work where the clear fabrication steps of RTD device and results are described.

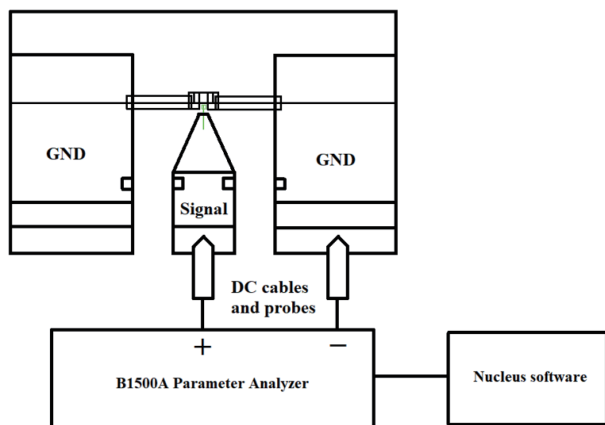

Fig. 5. (Color online) DC measurement setup for characterizing the fabricated RTD.

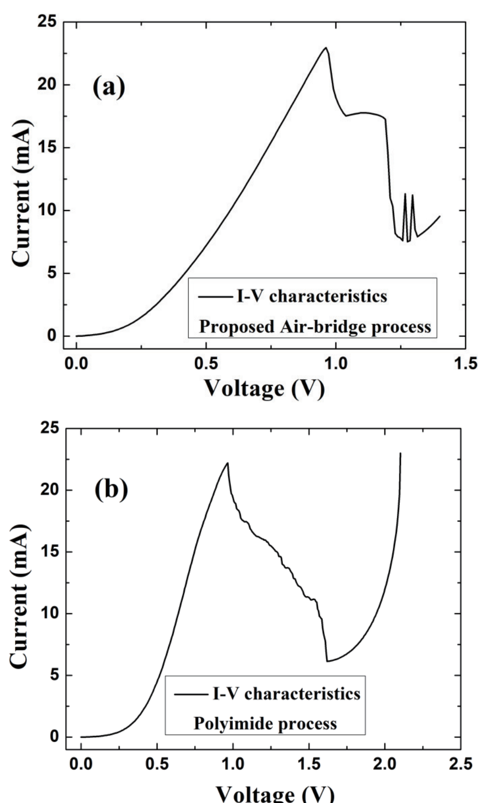

Fig. 6. Room temperature current–voltage characteristics of 4 × 4 μm^2 RTD device using (a) proposed air-bridge process, (b) polyimide process.

4. Conclusions and future perspectives

Double barrier quantum well resonant tunneling diode of active device area 4 × 4 μm^2 based on the InGaAs/AlAs system is developed using a novel air-bridge process. Current–voltage characteristics at room temperature for this device results in a peak-to-valley current ratio of 3.02 and a peak current density of 143.46 kA/cm^2. The measured results nearly match with the polyimide process with similar device dimension. This novel fabrication process may be extended to other material systems.

Acknowledgment

The authors would like to acknowledge James Watt Nanofabrication Centre (JWNC) staff, University of Glasgow, UK for the support related to device fabrication. Additionally, the work was funded by Horizon 2020 Future and Emerging Technologies ChipAI project under the grant agreement 828841.

Table 1. Comparison of DC characteristics for a 4 × 4 μm^2 RTD fabricated using the air-bridge and polyimide processes.

Parameter	Polyimide process	Proposed air-bridge process
Peak current, I_p (mA)	22.2	23
Valley current, I_v (mA)	6.2	7.6
Peak-valley current difference, ΔI (mA)	16.1	15.4
Peak voltage, V_p (V)	0.97	0.96
Valley voltage, V_v (V)	1.62	1.26
Peak-valley voltage difference, ΔV (V)	0.65	0.3
Peak-to-valley current ratio, PVCR	3.6	3
Peak current density, J_p (kA/cm^2)	139	143

Table 2. Performance comparison of InGaAs/AlAs RTD device fabricated by air-bridge process found in the literature and in our proposed method.

Parameter						Ref.
Active device area (μm^2)	DBQW			PVCR	J_p (kA/cm^2)	
	$t_{barrier}$ (nm)	t_{well} (nm)	$t_{barrier}$ (nm)			
4 × 4	1.3	4.5	1.3	3.2	260	[29]
3 × 3	1.2	4.5	1.2	8.35	40.9	[30]
8 × 8	3.0	5.1	2.8	8.6	24.6	[31]
176	2.0	4.0	2.0	43	24	[32]
4 × 4	–	–	–	1.2	250	[28]
4 × 4	1.4	4.5	1.4	3	143	This work

References

[1] Sun J P, Haddad G I, Mazumder P, et al. Resonant tunneling diodes: Models and properties. Proc IEEE, 1998, 86, 641

[2] Sugiyama H, Yokoyama H, Teranishi A, et al. Extremely high peak current densities of over 1 × 10^6 A/cm^2 in InP-based InGaAs/AlAs resonant tunneling diodes grown by metal–organic vapor-phase epitaxy. Jpn J Appl Phys, 2010, 49, 051201

[3] Shimizu N, Shinagawa M, Yamamoto M, et al. $In_{0.53}Ga_{0.47}As/AlAs$ resonant tunnelling diodes with switching time of 1.5 ps. Electron Lett, 1995, 31, 1695

[4] Smet J H, Broekaert T P E, Fonstad C G. Peak-to-valley current ratios as high as 50 : 1 at room temperature in pseudomorphic $In_{0.53}Ga_{0.47}As/AlAs/InAs$ resonant tunneling diodes. J Appl Phys, 1992, 71, 2475

[5] Huang C I, Paulus M J, Bozada C A, et al. AlGaAs/GaAs double barrier diodes with high peak-to-valley current ratio. Appl Phys Lett, 1987, 51, 121

[6] Al-Khalidi A, Alharbi K H, Wang J, et al. Resonant tunneling diode terahertz sources with up to 1 mW output power in the *J*-band. IEEE Trans THz Sci Technol, 2020, 10, 150

[7] Feiginov M, Sydlo C, Cojocari O, et al. Resonant-tunnelling-diode oscillators operating at frequencies above 1.1 THz. Appl Phys Lett, 2011, 99, 233506

[8] Asada M, Suzuki S. Room-temperature oscillation of resonant

tunneling diodes close to 2 THz and their functions for various applications. J Infrared Millim Terahertz Waves, 2016, 37, 1185
[9] Maekawa T, Kanaya H, Suzuki S, et al. Oscillation up to 1.92 THz in resonant tunneling diode by reduced conduction loss. Appl Phys Express, 2016, 9, 024101
[10] Zhang W K, Watson S, Figueiredo J, et al. Optical direct intensity modulation of a 79GHz resonant tunneling diode-photodetector oscillator. Opt Express, 2019, 27, 16791
[11] Paoloni C, Basu R P, Billa L R, et al. Long-range millimeter wave wireless links enabled by traveling wave tubes and resonant tunnelling diodes. IET Microw Antennas Propag, 2020, 2110
[12] Maezawa K. Resonant tunneling diodes and their application to high-speed circuits. IEEE Compound Semiconductor Integrated Circuit Symposium, 2005, 97.
[13] Romeira B, Pessoa L, Salgado H, et al. Photo-detectors integrated with resonant tunneling diodes. Sensors, 2013, 13, 9464
[14] Pfenning A, Hartmann F, Langer F B, et al. Sensitivity of resonant tunneling diode photodetectors. Nanotechnology, 2016, 27, 355202
[15] Oshima N, Hashimoto K, Suzuki S, et al. Terahertz wireless data transmission with frequency and polarization division multiplexing using resonant-tunneling-diode oscillators. IEEE Trans Terahertz Sci Technol, 2017, 7, 593
[16] J. Wang J, Al-Khalidi A, Wang L, et al. 15-Gb/s 50-cm wireless link using a high-power compact III–V 84-GHz transmitter. IEEE Transactions on Microwave Theory and Techniques, 2018, 66, 4698
[17] Weng Q C, An Z H, Zhang B, et al. Quantum dot single-photon switches of resonant tunneling current for discriminating-photon-number detection. Sci Rep, 2015, 5, 1
[18] Pfenning A, Jurkat J, Naranjo A, et al. Resonant tunneling diode photon number resolving single-photon detectors. SPIE Optical Engineering + Applications Proc SPIE 11128, Infrared Remote Sensing and Instrumentation XXVII, 2019, 11128, 47
[19] Duan S K, Hu X F, Wang L D, et al. Resonant tunneling diodes-based cellular nonlinear networks with fault tolerance analysis. Math Probl Eng, 2013, 2013, 1
[20] Romeira B, Figueiredo J M L, Javaloyes J. NanoLEDs for energy-efficient and gigahertz-speed spike-based sub-λ neuromorphic nanophotonic computing. Nanophotonics, 2020, 9, 4149
[21] Ortega I, Piro O, Romeira B, et al. Bursting and excitability in neuromorphic resonant tunneling diodes. 2021 Conference on Lasers and Electro-Optics Europe & European Quantum Electronics Conference (CLEO/Europe-EQEC), Munich, Germany, 2021, 1
[22] Esaki L, Tsu R. Superlattice and negative differential conductivity in semiconductors. IBM J Res Dev, 1970, 14, 61
[23] Tsu R, Esaki L. Tunneling in a finite superlattice. Appl Phys Lett, 1973, 22, 562
[24] Chang L L, Esaki L, Tsu R. Resonant tunneling in semiconductor double barriers. Appl Phys Lett, 1974, 24, 593
[25] Tsuchiya M, Sakaki H, Yoshino J. Room temperature observation of differential negative resistance in an AlAs/GaAs/AlAs resonant tunneling diode. Jpn J Appl Phys, 1985, 24, L466
[26] Wang J, Al-Khalidi A, Alharbi K, et al. High performance resonant tunneling diode oscillators as terahertz sources. 2016 46th European Microwave Conference (EuMC), 2017, 341
[27] Wang J, Al-Khalidi A, Cornescu A, et al. Design, fabrication and characterisation of RTD terahertz oscillators. 2019 European Microwave Conference in Central Europe (EuMCE), 2019, 261
[28] Zawawi M A M, Sexton J, Missous M. Advanced InGaAs/AlAs RTD with high current density incorporating multi-bridge (air-bridge) emitter design. UK Semiconductor 2012 Conference, 2012, 7
[29] Muttlak S G, Abdulwahid O S, Sexton J, et al. InGaAs/AlAs resonant tunneling diodes for THz applications: An experimental investigation. IEEE J Electron Devices Soc, 2018, 6, 254
[30] Zawawi M A M. Advanced $In_{0.8}Ga_{0.2}As/AlAs$ resonant tunneling diodes for applications in integrated mm-waves MMIC oscillators. Ph. D Thesis, University of Manchester, 2015
[31] Han C L, Chen C, Zou P H, et al. InP-base resonant tunneling diodes. J Semicond, 2009, 30, 064001
[32] Wang W, Sun H, Teng T, et al. High peak-to-valley current ratio $In_{0.53}Ga_{0.47}As/AlAs$ resonant tunneling diode with a high doping emitter. J Semicond, 2012, 33, 124002

Swagata Samanta (FIETE, MIEEE) received her Ph.D degree from Indian Institute of Technology Kharagpur in 2018. She continued her research as a postdoctoral fellow at the Centre for Nano Science and Engineering, Indian Institute of Science Bangalore and then at James Watt School of Engineering, University of Glasgow, UK. Presently, she is an Assistant Professor in the Department of Electronics and Communication Engineering at SRM University, Andhra Pradesh, India. Her research interests are interdisciplinary and encompass a broad range of areas, including novel on-chip nanophotonic and nanoelectronic devices, integrated optics, neuromorphics, VLSI systems, image/video processing, and artificial intelligence.

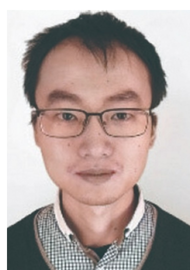

Jue Wang received his Ph.D degree in Electronics and Electrical Engineering in 2014 from the University of Glasgow, Glasgow, UK. Since 2014, he has been working on resonant tunneling diode based terahertz oscillator design as a Postdoctoral Researcher. His research interests include high-power terahertz devices and terahertz applications including wireless communications, imaging, etc.

Edward Wasige (S'97–M'99) received his B.Sc. (Eng.) degree in Electrical Engineering in 1988 from the University of Nairobi, Nairobi, Kenya, M.Sc. (Eng.) degree in microelectronic systems and telecommunications in 1990 from the University of Liverpool, Liverpool, UK, and Ph.D degree in Electrical Engineering from Kassel University, Kassel, Germany, in 1999. Prior to becoming a Lecturer with the University of Glasgow, Glasgow, UK, in 2002, he was a UNESCO Postdoctoral Fellow with the Technion—Israel Institute of Technology. His research interests include compound semiconductor micro-/nanoelectronics and applications with focus on gallium nitride electronics and resonant tunneling diode based terahertz electronics.